Electronic ladders with SO(5) symmetry: Phase diagrams and correlations at half filling

Holger Frahm and Martin Stahlsmeier
Institut für Theoretische Physik, Universität Hannover, D-30167 Hannover, Germany
(Received 29 September 2000; published 12 March 2001)

We construct a family of electronic-ladder models with SO(5) symmetry that have exact ground states in the form of finitely correlated wave functions. Extensions for these models preserving this symmetry are studied using these states in a variational approach. Within this approach, the zero-temperature phase diagram of these electronic ladders at half filling is obtained, reproducing the known results in the weak coupling (band insulator) and strong-coupling regime, first studied by Scalapino, Zhang, and Hanke. Finally, the compact form of the variational wave functions allows us to compute various correlation functions for these systems.

DOI: 10.1103/PhysRevB.63.125109 PACS number(s): 71.10.Pm, 71.10.Hf, 71.10.Fd

I. INTRODUCTION

The use of symmetries is an important tool to understand the effects of strong correlation in electronic systems. Recently, the SO(3) symmetry of the antiferromagnetic (AFM) order parameter has been combined with that of *d*-wave superconductivity to form a five-component-vector order parameter.[1] It has been argued that the low-energy sector of the resulting theory exhibits an approximate SO(5) symmetry that allows us to explain certain features such as the vicinity AFM order and superconductivity in the phase diagram of the high-T_c materials. Numerical diagonalization studies have been performed and the spectrum of low-lying excitations could in fact be classified according to this symmetry.

A complementary approach has been the attempt to construct microscopic electronic systems with manifest SO(5) invariance and studies of such models to extract the low-energy behavior. Scalapino, Zhang, and Hanke succeeded in constructing a two-chain ladder Hamiltonian of this type and studied the strong-coupling phase diagram of this system where they were able to identify several distinct phases (Ref. 2, referred to as SZH in the following). The properties of these systems at weak coupling in the metallic regime have been studied by means of bosonization.[3,4] Such ladder systems, particularly for magnetic insulators, have attracted much attention recently due to the existence of various experimental realizations in materials closely related to the high-T_c substances.[5] An interesting observation of Ref. 2 is the existence of an SO(5) superspin phase that has been studied in a variational approach based on finitely correlated matrix-product states similar to the ones used for $S=1$ Haldane magnets.[6–8] Finitely correlated states have also been considered in electronic systems to describe aspects of the phase diagram of extended Hubbard models[9,10] and other one-dimensional electronic models.[11,12]

For SU(2) spin systems the variational approach has been generalized to lattices with ladder geometry and proven to give access to large parts of their phase diagram.[13–16] This is the motivation for the present work where we extend the matrix-product states originally introduced in Ref. 2 to describe the strong-coupling physics of the SO(5) superspin phase. We construct manifestly SO(5)-invariant many-particle wave functions from matrices containing *all* 16 electronic states on a given rung of the electronic ladder. The relative weight of the six different SO(5) multiplets on a rung is controlled by free parameters that are used to perform a variational study of the zero-temperature phase diagram of the ladder at half filling. At strong coupling, the results known from Ref. 2 are reproduced within our approach. Furthermore, at weak coupling and sufficiently large interchain hopping amplitude $t_\perp$ the matrix-product state correctly describes the gapped ground state of a band insulator corresponding to a filled Fermi sea of electrons with one parity. For intermediate coupling we find a phase with finite amplitude of the SO(5)-spinor quartets that are essential for the presence of a metallic phase of the ladder. The compact form of the variational states allows us to study various correlation functions of interest.

In the following section we present the classification of the electronic states of a two-leg ladder system according to the SO(5) symmetry and discuss all possible SO(5)-symmetric single rung interactions. In Sec. III we review the SZH model and consider tensor products of rung states to include couplings of neighboring rungs. Section IV deals with various SO(5)-symmetric extensions of this model and a general construction routine for systems with exact finitely correlated ground states is given. Section V contains a detailed analysis of the ground-state phase diagram of the system in the case of weak and intermediate coupling within a variational approach based on such wave functions. Furthermore, we calculate the corresponding correlation functions within this approach. A summary of our results is given in Sec. VI.

II. ELECTRONIC STATES OF SO(5)-SYMMETRIC LADDER MODELS

We consider a two-chain electronic ladder model with canonical creation and annihilation operators $c^\dagger_\sigma(x), c_\sigma(x)$ for electrons (with spin-projection $\sigma=\uparrow,\downarrow$) on sites x of the upper leg and analogous operators $d^\dagger_\sigma(x), d_\sigma(x)$ for the electrons on the lower leg. In order to discuss the SO(5) symmetry of the ladder model and to classify all the 16 possible states on a rung according to this symmetry, these operators are combined into four-dimensional SO(5) spinors[2,17]

$$\Psi_\alpha(x)=(c_\uparrow(x),c_\downarrow(x),d^\dagger_\uparrow(x),d^\dagger_\downarrow(x))^T \quad (x \text{ even}) \quad (2.1)$$

and

$$\Psi_\alpha(x)=(d_\uparrow(x),d_\downarrow(x),c_\uparrow^\dagger(x),c_\downarrow^\dagger(x))^T \quad (x \text{ odd}). \quad (2.2)$$

Using this definition the ten local generators L_{ab} of the SO(5) algebra on a single rung x are defined as

$$L_{ab}(x)=-\frac{1}{2}\Psi_\alpha^\dagger(x)\Gamma_{\alpha\beta}^{ab}\Psi_\beta(x), \quad a,b=1,\ldots,5. \quad (2.3)$$

Here Γ^{ab} are ten antisymmetric, 4×4 matrices (their explicit form is given in Appendix A). A convenient basis of the Hilbert space on a single rung is diagonal in the quadratic Casimir charge

$$C(x)=\sum_{a<b} L_{ab}^2(x). \quad (2.4)$$

In addition we choose to diagonalize the total charge $Q=\frac{1}{2}(c^\dagger c+d^\dagger d-2)$ and the z component of the spin $S^z=\frac{1}{2}(c^\dagger\sigma_z c+d^\dagger\sigma_z d)$. Based on the eigenvalues of C the Hilbert space can be decomposed into six SO(5) multiplets.

(1) Three SO(5) singlets ($C=0$), for R see Eq. (A2),

$$|\Psi_{0,0}^{(1)}\rangle=|\Omega\rangle\equiv\frac{c_\uparrow^\dagger d_\downarrow^\dagger-c_\downarrow^\dagger d_\uparrow^\dagger}{\sqrt{2}}|0\rangle=\frac{1}{\sqrt{2}}\left(\left|\begin{matrix}\uparrow\\\downarrow\end{matrix}\right\rangle-\left|\begin{matrix}\downarrow\\\uparrow\end{matrix}\right\rangle\right),$$

$$|\Psi_{0,0}^{(2)}\rangle=\frac{1}{\sqrt{8}}\Psi_\alpha R_{\alpha\beta}\Psi_\beta|\Omega\rangle\sim\left|\begin{matrix}\uparrow\downarrow\\-\end{matrix}\right\rangle, \quad (2.5)$$

$$|\Psi_{0,0}^{(3)}\rangle=\frac{1}{\sqrt{8}}\Psi_\alpha^\dagger R_{\alpha\beta}\Psi_\beta^\dagger|\Omega\rangle\sim\left|\begin{matrix}-\\\uparrow\downarrow\end{matrix}\right\rangle.$$

(2) An SO(5) vector quintet ($C=4$) containing the ferromagnetically polarized state at half filling

$$|\Psi_{5,\alpha}^{(1)}\rangle\in\left\{\left|\begin{matrix}-\\-\end{matrix}\right\rangle,\left|\begin{matrix}\uparrow\downarrow\\\uparrow\downarrow\end{matrix}\right\rangle,\left|\begin{matrix}\uparrow\\\uparrow\end{matrix}\right\rangle,\left|\begin{matrix}\downarrow\\\downarrow\end{matrix}\right\rangle,\left|\begin{matrix}\uparrow\\\downarrow\end{matrix}\right\rangle+\left|\begin{matrix}\downarrow\\\uparrow\end{matrix}\right\rangle\right\},$$
$$\alpha=1,\ldots,5. \quad (2.6)$$

(3) Two SO(5) spinor quartets ($C=5/2$) for an odd number of electrons on a given rung

$$|\Psi_{4,\alpha}^{(1)}\rangle\sim\sqrt{2}\Psi_\alpha|\Omega\rangle\in\left\{\left|\begin{matrix}-\\\uparrow\end{matrix}\right\rangle,\left|\begin{matrix}-\\\downarrow\end{matrix}\right\rangle,\left|\begin{matrix}\uparrow\\\uparrow\downarrow\end{matrix}\right\rangle,\left|\begin{matrix}\downarrow\\\uparrow\downarrow\end{matrix}\right\rangle\right\},$$
$$\alpha=1,\ldots4, \quad (2.7)$$

$$|\Psi_{4,\alpha}^{(2)}\rangle\sim\sqrt{2}\Psi_\alpha^\dagger|\Omega\rangle\in\left\{\left|\begin{matrix}\uparrow\\-\end{matrix}\right\rangle,\left|\begin{matrix}\downarrow\\-\end{matrix}\right\rangle,\left|\begin{matrix}\uparrow\downarrow\\\uparrow\end{matrix}\right\rangle,\left|\begin{matrix}\uparrow\downarrow\\\downarrow\end{matrix}\right\rangle\right\},$$
$$\alpha=1,\ldots4.$$

We label the states $|\Psi_{d,\alpha}^{(k)}\rangle$ on a rung by the dimension d of the corresponding multiplet ($\alpha=1,\ldots,d$) and an additional index k. Similarly, we can characterize product states on two rungs (see Sec. III). Alternatively, the vector quintet (2.6) can be constructed from SO(5) spinors $|\Psi_{5,1(2)}^{(1)}\rangle=(1/\sqrt{2})(n_1\pm n_5)|\Omega\rangle$, $|\Psi_{5,3(4)}^{(1)}\rangle=(1/\sqrt{2})(n_2\pm n_3)|\Omega\rangle$ and $|\Psi_{5,5}^{(1)}\rangle=n_4|\Omega\rangle$ with the superspin vector

$$n^a(x)\equiv\frac{1}{2}\Psi_\alpha^\dagger(x)\Gamma_{\alpha\beta}^a\Psi_\beta(x), \quad a=1,\ldots,5. \quad (2.8)$$

Again, the explicit form of the 4×4 Dirac Γ matrices Γ^a is given in Appendix A.

Any electronic ladder model with a local SO(5)-symmetry on a rung has to preserve the degeneracy of the energy within the states of each single multiplet. The invariant Hamiltonian on a single rung can therefore be written as a sum over projection operators on these states:

$$h_x=\lambda_5\sum_{\mu=1}^{5}|\Psi_{5,\mu}^{(1)}\rangle\langle\Psi_{5,\mu}^{(1)}|+\sum_{k,l=1}^{2}\lambda_4^{(k,l)}\sum_{\mu=1}^{4}|\Psi_{4,\mu}^{(k)}\rangle\langle\Psi_{4,\mu}^{(l)}|$$
$$+\sum_{k,l=1}^{3}\lambda_0^{(k,l)}|\Psi_{0,0}^{(k)}\rangle\langle\Psi_{0,0}^{(l)}|, \quad (2.9)$$

where $\lambda_d^{(k,l)}=(\lambda_d^{(l,k)})^*$ because of the hermiticity of h_x. All SO(5)-symmetric terms on a rung can be expressed using linear combinations of these projection operators, e.g., the projection operator on the first singlet $|\Psi_{0,0}^{(1)}\rangle$ is

$$\hat{P}_{0,0}^{1,1}=|\Psi_{0,0}^{(1)}\rangle\langle\Psi_{0,0}^{(1)}|=-\tfrac{1}{3}\vec{S}_c(x)\vec{S}_d(x)+\tfrac{4}{3}[\vec{S}_c(x)\vec{S}_d(x)]^2, \quad (2.10)$$

with $\hat{P}_{d,\mu}^{k,l}=|\psi_{d,\mu}^{(k)}\rangle\langle\psi_{d,\mu}^{(l)}|$ and $\vec{S}_c(x)=\frac{1}{2}c^\dagger(x)\vec{\sigma}c(x)$. A complete classification of these terms is given in Appendix B. As a simple example we choose

$$\lambda_0=\begin{pmatrix}-\frac{7}{2}U-3V & 2\sqrt{2}t_\perp & -2\sqrt{2}t_\perp\\ & \frac{U}{2}-V & 0\\ * & & \frac{U}{2}-V\end{pmatrix},$$

$$\lambda_4=\begin{pmatrix}0 & -2t_\perp\\ * & 0\end{pmatrix}, \quad \text{and} \quad \lambda_5=\frac{U}{2}+V,$$

which leads to the Hubbard-type Hamiltonian[2] with an SO(5)-symmetry introduced by SZH

$$H_{rung}=H_{Coulomb}+H_{Hopping}$$
$$=\sum_x\ (U\{[n_{c\uparrow}(x)-\tfrac{1}{2}][n_{c\downarrow}(x)-\tfrac{1}{2}]+(c\to d)\}$$
$$+V[n_c(x)-1][n_d(x)-1]+J\vec{S}_c(x)\vec{S}_d(x)$$
$$-2t_\perp[c_\sigma^\dagger(x)d_\sigma(x)+\text{H.c.}]), \quad (2.11)$$

where $J=4(U+V)$. This condition on the exchange amplitude guarantees the degeneracy between the states in the SO(5) quintet and therefore the local SO(5) symmetry of the

system. We will discuss this model and SO(5)-symmetric extensions in the following sections.

III. COUPLING OF NEIGHBORING RUNGS

In order to describe an extended quasi-one-dimensional electronic system one has to include coupling of neighboring rungs in addition to single-rung interactions considered in the previous section. The simplest possible term is an SO(5)-symmetric hopping term between adjacent rungs

$$-2t_{\parallel}\sum_{\langle x,y\rangle}[c_{\sigma}^{\dagger}(x)c_{\sigma}(y)+d_{\sigma}^{\dagger}(x)d_{\sigma}(y)+\text{H.c.}], \quad (3.1)$$

which can be brought into a manifestly SO(5)-symmetric form using the alternating definitions of the spinors (2.1) and (2.2). This hopping term together with the local-rung interactions (2.11) yield the complete SZH model.[2] The ground-state phase diagram of this system in the limit of strong coupling ($U,V \gg t_{\perp},t_{\parallel}$) has been determined by SZH using perturbation theory (see Fig. 2). Four different phases have been established at half filling.

In phase I (occurring for $0 \leqslant V \leqslant -2U$) the model can be mapped onto an Isinglike system in a magnetic field: phase I_a ($V \geqslant -U/3$) is a charge-density wave (CDW) phase and I_b ($V \leqslant -U/3$) corresponds to the disordered Ising phase. Phase II is a spin-gap d-wave phase (product of rung singlets), emerging for $V \geqslant -U, U \geqslant 0$ and for $V \geqslant -2U, U \leqslant 0$. The phase III ($V \leqslant -U, V \leqslant 0$) is the superspin phase where the SO(5) quintet is dominant. For a further examination of this superspin phase, SZH have used the finitely correlated wave function

$$|\Psi_0^{SZH}\rangle = \mathrm{Tr}\left(\prod_{x=1}^{L}\Gamma^a n_a|\Omega\rangle\right) \quad (3.2)$$

(summation over the index a is implied and the trace is taken in the 4×4 matrix space where the Γ^a are defined). In this form periodic boundary conditions have been imposed. By adding many particle interactions to their original Hubbard-type Hamiltonian, this state (3.2) can be made to be the exact ground state of the resulting model. This state has been argued to capture the essential physics of the superspin phase—similar to the role of the AKLT-model as a representative for a Haldane-gapped spin-1 chain. The wave function (3.2) will be the starting point for constructing a generalized matrix product wave function including all 16 states on a rung (see Sec. IV) and later be used for a variational study of the ground-state phase diagram of the SZH model and its various SO(5) symmetric extensions beyond strong coupling (see Sec. V). The hopping term (3.1) is one of many possibilities to include interactions between two adjacent rungs of the ladder but the requirement for a local SO(5) symmetry puts constraints on the explicit form of these terms. Explicit expressions for some of the interaction terms are listed in terms of electron operators in Appendix B. For a classification of these additional interactions we consider products of wave functions on two neighboring rungs x and y. A decomposition into SO(5) multiplets similar to (2.5)–(2.7) gives 50 different multiplets invariant under the action of the SO(5) generators $\mathcal{L}_{ab}(x,y)=L_{ab}(x)+L_{ab}(y)$. Tensor products containing a singlet factor on one of the rungs are trivial leading to simple product states, e.g., the SO(5) singlets $|\Psi_{0,0}^{(i)}\rangle_x|\Psi_{0,0}^{(j)}\rangle_y$. Altogether there are nine singlets, 12 quartets and six quintets of this form. The remaining 169 states are obtained by forming tensor products of quartets (2.7) and quintets (2.6). The decomposition of these products into irreducible representations of SO(5) reads

$$\mathbf{4}\otimes\mathbf{4}=\mathbf{1}\oplus\mathbf{5}\oplus\mathbf{10},$$

$$\mathbf{4}\otimes\mathbf{5}=\mathbf{4}\oplus\mathbf{16},$$

$$\mathbf{5}\otimes\mathbf{5}=\mathbf{1}\oplus\mathbf{10}\oplus\mathbf{14}$$

[numbers denote the dimension of the corresponding SO(5) irrep]. For example, one of four SO(5) singlets in the tensor product of quartet states (2.7) is

$$|\Psi_{0,0}^{(10)}(x,y)\rangle \equiv \frac{1}{2}(-|\Psi_{4,1}^{(1)}\rangle|\Psi_{4,3}^{(2)}\rangle-|\Psi_{4,2}^{(1)}\rangle|\Psi_{4,4}^{(2)}\rangle + |\Psi_{4,3}^{(1)}\rangle|\Psi_{4,1}^{(2)}\rangle+|\Psi_{4,4}^{(1)}\rangle|\Psi_{4,2}^{(2)}\rangle). \quad (3.3)$$

Similar combinations of the rung states appear in the other states, the Casimir charges of the new multiplets are $C=6$ for the decuplets, $C=10$ for the 14-dimensional and $C=15/2$ for the 16-dimensional representations. The multiplets can be classified further according to the different eigenvalues of Q and S^z on their member states. In Fig. 1 the state content of the various multiplets is shown. In the following we use this classification of the SO(5) multiplets to construct ladder systems with exact ground states including different SO(5) symmetric nearest-neighbor interactions.

IV. EXTENSIONS OF SZH

As mentioned in the Introduction the finitely correlated wave functions originally introduced to discuss the spin-liquid phases arising in one-dimensional higher-spin Heisenberg models[6–8] have recently been generalized to more general lattices. In particular, ladder models whose ground states are of this form have been constructed.[13,18,19] In these spin systems the ground state is of the form $|\Psi_0\rangle=\Pi_{x=1}^{L}g_x$ where g_x is a (2×2) matrix containing the different states on a single site or rung x (e.g., spin-1 states for the AKLT model, singlet and triplet states for a two-leg $S=1/2$ ladder, etc.). Different properties under translation in the extended direction can be realized by an appropriate choice of the free parameters appearing in g_x (e.g., an alternation to introduce dimerization[18,20,21]). Within a transfer matrix approach, it is straightforward to compute various ground-state correlation functions for different boundary conditions, periodic ones correspond to taking the trace of the matrix-product wave function.[22]

For a further analysis of the SZH model and the construction of SO(5)-symmetric ladder systems with exact ground states in matrix product form, we have extended the wave

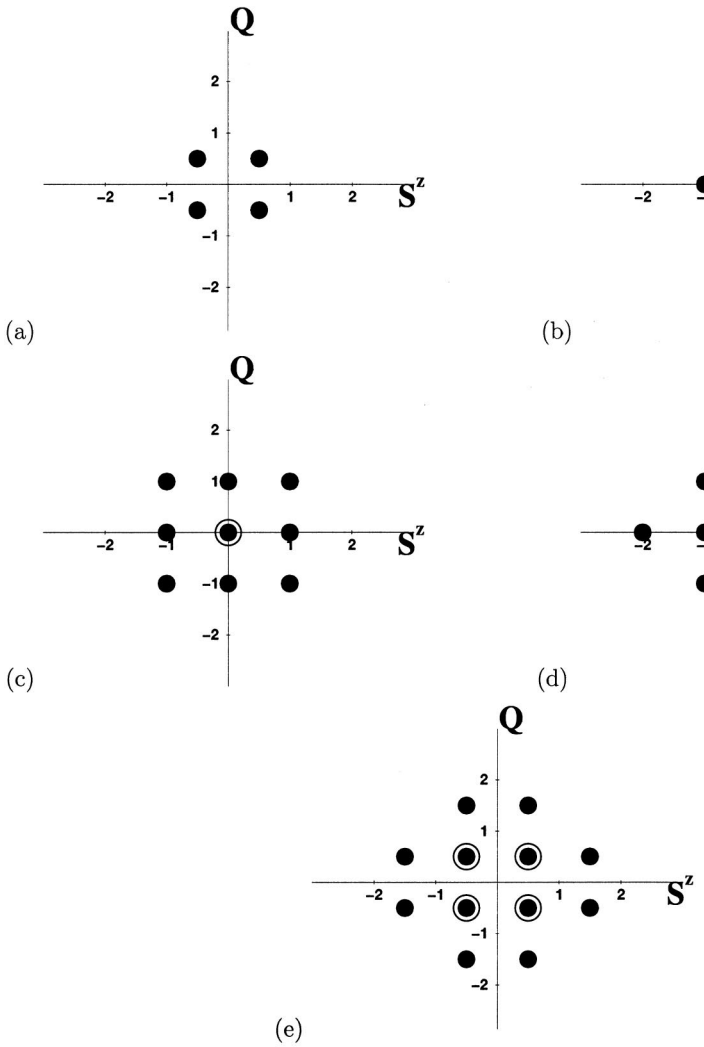

FIG. 1. The irreducible SO(5) representations appearing on a pair of rungs decomposed corresponding to the eigenvalues of Q and S^z: (a) the quartet (with Casimir charge $C=5/2$), (b) the quintet ($C=4$), (c) the ten-dimensional ($C=6$), (d) the 14-dimensional ($C=10$), and (e) 16-dimensional ($C=15/2$) irrep (double circle indicate two states with identical eigenvalues).

function (3.2) to include the three SO(5) singlets (2.5) and the two SO(5) spinor quartets (2.7)

$$|\Psi_0\rangle = \mathrm{Tr}\left(\prod_{x=1}^{L} g_x(\{p_i\}) \right). \tag{4.1}$$

Now g_x is a 5×5 matrix and p_i ($i=1,\ldots,6$) are variational parameters assigning different weights to the multiplets (2.5)–(2.7) on a rung (see Appendix A). We restrict ourselves to the translational invariant case, where the parameters p_i are chosen to be independent of the rung position x. In this case the matrix-product wave function on two neighboring rungs contains two SO(5) singlets, two quartets, one quintet, and one decuplet. The 14-dimensional and 16-dimensional representations are absent by construction. The states of the matrix product are linear combinations of the basis in Sec. III above, their explicit form is rather complicated. With respect to the spin-SU(2) subalgebra the remaining multiplets present in the matrix product contain spin singlet, doublet, and triplet states only (states with total spin polarization $S^z>1$ are members of the 14- and 16-dimensional representations, see Fig. 1). An immediate consequence is that the ansatz cannot be expected to describe the formation of ferromagnetic domains with higher spin states. An analogous argument holds for higher values of the charge Q, corresponding to strong local deviations from half filling.

There is a simple way to construct spin-ladder systems with matrix-product wave functions as ground states[13] and a generalization to electronic-ladder models with an SO(5) symmetry is straightforward. The starting point is a general SO(5)-symmetric Hamilton operator on two neighboring rungs

$$\begin{aligned} h_{x,x+1} = & \sum_{k,l=1}^{4} \lambda_{16}^{(k,l)} \sum_{\mu=1}^{16} \hat{P}_{16,\mu}^{k,l} + \sum_{\mu=1}^{14} \lambda_{14} \hat{P}_{14,\mu} \\ & + \sum_{k,l=1}^{5} \lambda_{10}^{(k,l)} \sum_{\mu=1}^{10} \hat{P}_{10,\mu}^{k,l} + \sum_{k,l=1}^{10} \lambda_{5}^{(k,l)} \sum_{\mu=1}^{5} \hat{P}_{5,\mu}^{k,l} \\ & + \sum_{k,l=1}^{16} \lambda_{4}^{(k,l)} \sum_{\mu=1}^{4} \hat{P}_{4,\mu}^{k,l} + \sum_{k,l=1}^{14} \lambda_{0}^{(k,l)} \hat{P}_{0,0}^{k,l}, \end{aligned} \tag{4.2}$$

where $\hat{P}_{d,\mu}^{k,l} = |\psi_{d,\mu}^{(k)}\rangle\langle\psi_{d,\mu}^{(l)}|$ are projection operators on all possible SO(5) multiplets (see Sec. III). The states $|\psi_{d,\mu}^{(k)}\rangle$ are

product wave functions on two rungs, k and l label the multiplet, μ the states in the multiplet, and d is the corresponding dimension of this irreducible representation. The hermiticity of $h_{x,x+1}$ requires $\lambda_d^{(k,l)}=(\lambda_d^{(l,k)})^*$ for the coupling constants, leaving altogether 322 free parameters in the Hamiltonian. A Hamiltonian $H=\Sigma_x h_{x,x+1}$ has a finitely correlated ground state $|\Psi_0\rangle=\Pi_x g_x$ with zero energy provided that the following conditions are satisfied:[13] (1) $h_{x,x+1}$ has to annihilate all states contained in the matrix elements of the product $g_x g_{x+1}$, (2) all other eigenstates of $h_{x,x+1}$ have positive energy. Starting with an ansatz for g_x in Eq. (4.1), one has to identify all multiplets $|\psi_{d,\mu}^{(i_d)}\rangle$ contained in the product wave function $g_x g_{x+1}$. These multiplets are labeled by indices $i_d=1,\ldots,g_d$ where the maximum number g_d is the number of multiplets with an equal Casimir charge (d is the dimension of the irreducible representation), e.g., $g_{10}=2$ if the product wave function on two neighboring rungs contains two independent SO(5) decuplets. After the determination of the multiplet content of $|\Psi_0\rangle$ the corresponding parameters $\lambda_d^{(k,i_d)}$ in $h_{x,x+1}$ are set to zero to fulfill the first condition. The remaining operators in Eq. (4.2) will now project on states not included in the matrix-product wave function, which leads to zero energy for the ansatz. To satisfy now the second condition, the reduced matrices $\lambda_d^{(k,l)}$ ($l\neq i_d$) have to be chosen positive definite (i.e., positive eigenvalues) such that Eq. (4.1) will be the lowest energy state of the system.

In principle a general Hamiltonian, where our ansatz (4.1) is the exact ground state, can be built by operators projecting on the other remaining SO(5) multiplets (e.g., the 14-dimensional and the four 16-dimensional representations) and it has 249 free coupling constants $\lambda_d^{(k,l)}$ ($l\neq i_d$). We give explicit expressions for some of these operators in terms of electron operators in Appendix B 3. In general, however, the structure of these projection operators is quite complicated making it difficult to motivate these exactly solvable systems on physical grounds.

V. VARIATIONAL STUDIES OF THE PHASE DIAGRAM

An examination of the SZH model beyond strong coupling can be done by using Eq. (4.1) as a variational wave function. This wave function leads to the variational energy

$$E_{rung}=\langle\Psi_0|H_{Coulomb}|\Psi_0\rangle \sim (p_2^2+p_3^2)(U/2-V)+5p_6^2(U/2+V)-p_1^2(\tfrac{7}{2}U+3V) \tag{5.1}$$

for spin and charge interaction on a rung [see Eq. (2.11)]. Here p_6 is the parameter corresponding to the SO(5) quintet, p_1 is the weight of the singlet $|\Omega\rangle$ and $p_{2,3}$ of the symmetric and antisymmetric linear combinations of the other SO(5) singlets (2.5). The variational energy corresponding to the hopping term on a rung is

$$E_{t_\perp}=\langle\Psi_0|H_{Hopping}|\Psi_0\rangle\sim t_\perp\left[8p_1p_2+2\left(\frac{p_5^2-p_4^2}{h_2}\right)(w-h_1)\right] \tag{5.2}$$

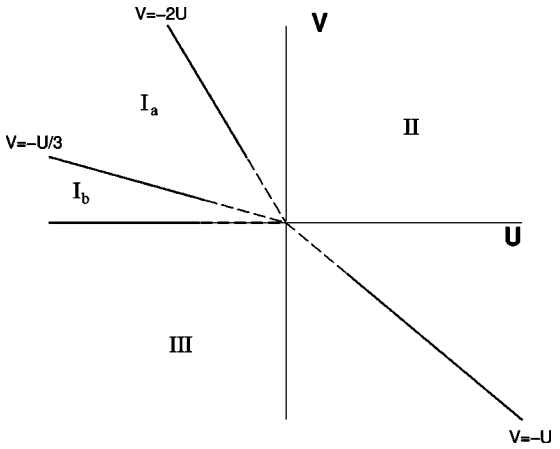

FIG. 2. Strong-coupling phase diagram, U and V measured in units of $t_\parallel$.

and between two neighboring rungs [see Eq. (3.1)] it is

$$E_{t_\parallel}\sim t_\parallel[p_4p_5(25p_6^2+p_1^2-p_2^2-p_3^2)+h_2(p_2p_3-5p_1p_6) +(p_4^2-p_5^2)(5p_2p_6-p_1p_3)], \tag{5.3}$$

where $h_1=5p_6^2+p_1^2+p_2^2+p_3^2$, $h_2=p_4^2+p_5^2$ and $w=\sqrt{h_1^2+16h_2^2}$.

In the strong coupling limit one can neglect these hopping terms (5.2) and (5.3). Minimizing the energy with respect to the p_i reproduces exactly the phase diagram calculated by SZH within perturbation theory (Fig. 2) where the phases are fixed by the largest amplitude p_i of the corresponding state and the crossover is continuous. Phase I is dominated by the bonding singlet state with amplitude p_2, phase III is the superspin phase (p_6), and phase II consists of products of rung singlets (p_1). In this approach with translationally invariant p_i the crossover between the two Ising-phases cannot be reproduced. We now extend this analysis of the phase diagram of the SZH model to weak and intermediate coupling.

A. Weak coupling phase diagram

The band structure of the noninteracting system at half filling is well known. For $U=V=0$ there are two energy bands, given by

$$\epsilon_\pm(k)=\pm 2t_\perp-4t_\parallel\cos(k),\quad -\pi\leqslant k\leqslant\pi \tag{5.4}$$

and two different cases have to be distinguished.

For $t_\perp<2t_\parallel$ the Fermi energy intersects the two bands [see Fig. 3(a)] and for $t_\perp\geqslant 2t_\parallel$ they are separated by an energy gap [see Fig. 3(b)]. The gapless system ($t_\perp<2t_\parallel$) has been studied using bosonization of the low-lying modes in the vicinity of the four Fermi points to obtain the phase diagram for weak coupling ($U,V\ll t_\perp,t_\parallel$): Lin *et al.*[4] found that at half filling the system is driven toward an integrable SO(8)-symmetric Gross-Neveu model in a weak-coupling renormalization-group analysis and predicted the occurrence of additional phases compared to the strong-coupling case. The ongoing debate on these results (see the criticism of Ref. 23) cannot be clarified within the present ansatz: Using fi-

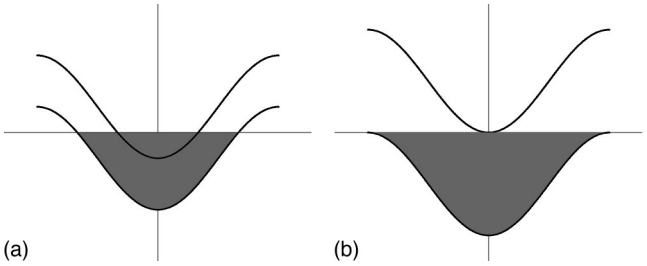

FIG. 3. Band structure of a two-leg ladder model for (a) $t_\perp = t_\parallel$ and (b) $t_\perp = 2t_\parallel$.

nitely correlated wave functions always leads to an exponential decay of correlation functions, indicating the existence of an energy gap between the ground state and the first excited state.

B. Phase diagram for $t_\perp \geqslant 2t_\parallel$

For $t_\perp \geqslant 2t_\parallel$ the variational ansatz gives the exact ground state for the noninteracting system ($U=V=0$).

Choosing $p_1 = -(1/\sqrt{2})$, $p_2 = (1/\sqrt{2})$, and $p_i \equiv 0$ for $i = 3, \ldots, 6$ we find

$$|\Psi_0\rangle \sim \prod_{x=1}^{L} (-c_\uparrow^\dagger d_\downarrow^\dagger + c_\downarrow^\dagger d_\uparrow^\dagger - d_\uparrow^\dagger d_\downarrow^\dagger - c_\uparrow^\dagger c_\downarrow^\dagger)(x)|0\rangle, \tag{5.5}$$

which corresponds to complete filling of the modes with energy $\epsilon_-(k)$ in Eq. (5.4), the band insulator. Consequently, we expect the variational approach to give reasonable results for the weak-coupling phase diagram in this regime of hopping amplitudes. The quality of the approach can be measured by the mean deviation $\sqrt{\langle (\Delta H)^2 \rangle} = \sqrt{\langle H^2 \rangle - \langle H \rangle^2}$ of the energy. For $U, V \ll t_\perp, t_\parallel$ the mean deviation stays small compared to the energy so that the ansatz should give reliable results.

We find that only two phases are present in the weak-coupling case (see Fig. 4): the Ising phase I (p_2) and the spin-gap d-wave phase II (p_1) already known from the strong-coupling diagram (see Fig. 2). The superspin phase disappears and also the SO(5) quartets have no significant weight ($p_4, p_5, p_6 \sim 0$) as expected for a band insulator.

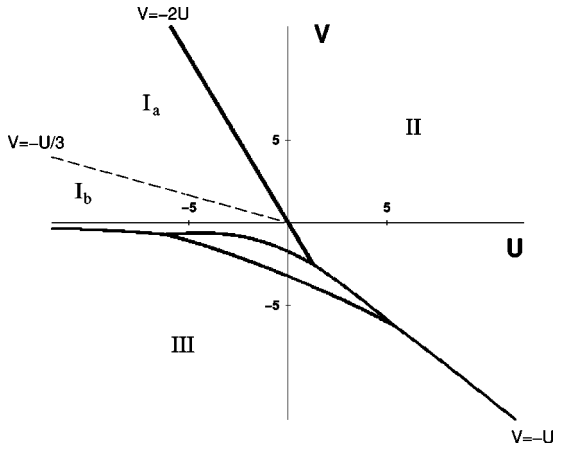

FIG. 4. Phase diagram for $t_\perp = 2t_\parallel$ ($t_\parallel = 1$): the phase boundaries were calculated by comparing the amplitudes of the different multiplets.

Considering the complete ground-state phase diagram (see Fig. 4) we find an additional phase for intermediate coupling ($U, V \cong t_\perp, t_\parallel$) where the SO(5) quartets have the largest weight, in particular the rung-symmetric one $|Q_\alpha^+\rangle$ (A5). Apart from these, the symmetric singlet state $(\Psi_\alpha^\dagger R_{\alpha\beta} \Psi_\beta^\dagger - \Psi_\alpha R_{\alpha\beta} \Psi_\beta)|\Omega\rangle$—which determines the ground state in phase I—has a significant weight. Due to the resonating structure of the ansatz and the relatively large variational value of $\langle (\Delta H)^2 \rangle$ the phase boundaries are not very accurate—for a more detailed study of this question the present work should be complemented by a numerical approach. As discussed earlier, it is not possible within this approach to determine the position of the crossover line between the two Ising phases, or even whether this transition still occurs for the case of weak or intermediate coupling.

C. Ground-state correlations

The physics in the ground state is determined by ground-state correlation functions, which are easily computed from matrix-product wave functions. The matrix-product ansatz (4.1) with the six free parameters p_i represents the ground state for a large class of models. We have calculated various correlation functions explicitly in the thermodynamic limit ($L \to \infty$) for this variety of models (a detailed list is given in Appendix C) and we determined the correlation length and the amplitude of different ground-state correlations for the SZH model when we used the ansatz as a variational wave function.

The two-point correlations in matrix-product states are always short-ranged (if not vanishing) and have the following form:

$$\langle O^\dagger(r) O(0) \rangle = A(\{p_i\}) e^{-r/\xi}.$$

They exhibit an exponential decay with the correlation length ξ and amplitude $A(\{p_i\})$. As an example, we consider the correlation length and amplitude of the expectation value of the spin-spin correlation function $\langle \vec{S}_{c,d}(r) \vec{S}_{c,d}(0) \rangle$ (see Fig. 5) and of field correlators $\langle c_\alpha^\dagger(r) c_\beta(0) \rangle$, $\alpha, \beta \in \{g, u\}$ (Fig. 6) for the SZH model on a circle in the U-V-plane (with $U^2 + V^2 = 3$) intersecting the phases I,II and the quartet phase (see Fig. 4).

The spin-spin correlation function $\langle \vec{S}_{c,d}(r) \vec{S}_{c,d}(0) \rangle$ in Fig. 5 is nonvanishing only in the quartet phase but with an extremely small correlation length indicating strong nearest neighbor correlations. For the electron-electron correlation in Fig. 6 with $c_{g,u}(x) = [c_\uparrow(x) + c_\downarrow(x)] \pm [d_\uparrow(x) + d_\downarrow(x)]$ the correlation length ξ is small for all angles ϕ but with a very large amplitude A except in the quartet phase.

The sharp peak in both diagrams at $\phi \sim \frac{5}{8}\pi$ indicates the crossover of the phases II and I in Fig. 4 where the correlation length diverges. Calculating these correlations in the strong-coupling limit, the phase boundaries in Fig. 4 are denoted by very sharp peaks in the electron-electron correlation length $\xi_{\langle c_{g,u}^\dagger(r) c_{g,u}(0) \rangle}$ with a nonvanishing amplitude. The

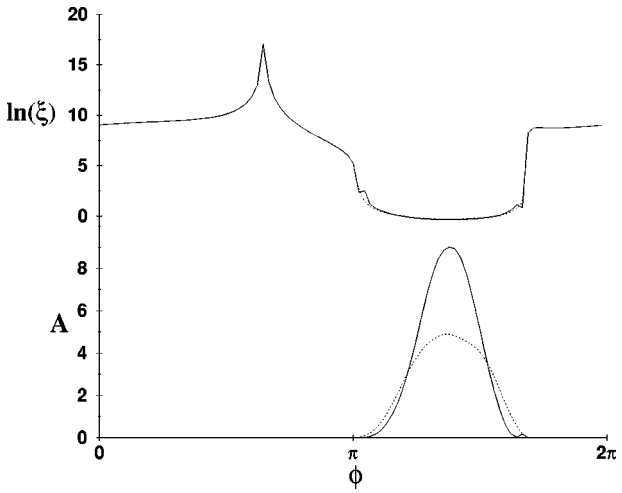

FIG. 5. Correlation length and amplitude for the spin-spin correlation function, the full line corresponds to $\langle \vec{S}_{c(d)}(r)\vec{S}_{c(d)}(0)\rangle$ and the dotted line to $\langle \vec{S}_{c(d)}(r)\vec{S}_{d(c)}(0)\rangle$.

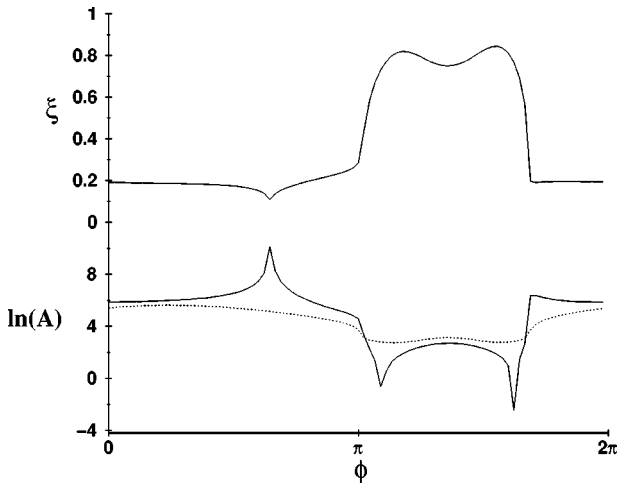

FIG. 6. The correlation length and amplitude of the expectation value $\langle c^{\dagger}_{g,u}(r)c_{g,u}(0)\rangle$, the full line corresponds to $\langle c^{\dagger}_{g(u)}(r)c_{g(u)}(0)\rangle$ and the dotted line to $\langle c^{\dagger}_{g(u)}(r)c_{u(g)}(0)\rangle$.

spin-spin correlations are zero in the whole phase diagram and give no further hints of an underlying structure in the system.

D. Variational examination of SO(5)-symmetric extensions

Our variational approach is also suitable to study the phase diagrams of various SO(5)-symmetric extensions of the SZH model. We have considered additional interactions on a single rung and between two neighboring rungs, using the construction routine of Secs. II and IV.

1. Single-rung interactions

All single-rung interactions can be constructed using the projection operators of Sec. II and a detailed list of all possible terms can be found in the Appendix B. Taking into account the operators $\hat{P}^{k,l}_{d,\mu}$ with the coupling constants $\lambda^{(k,l)}_{d}$ leads to the following contributions to the variational energy (5.1), calculated with the ansatz (4.1):

$$\langle \hat{P}^{1,1}_{(0,0)}\rangle = \frac{p_1^2}{w}, \tag{5.6a}$$

$$\langle \hat{P}^{2,2}_{(0,0)}\rangle = \frac{1}{2w}(p_2+p_3)^2, \tag{5.6b}$$

$$\langle \hat{P}^{3,3}_{(0,0)}\rangle = \frac{1}{2w}(p_2-p_3)^2, \tag{5.6c}$$

$$\langle \hat{P}^{1,2}_{(0,0)}+\hat{P}^{2,1}_{(0,0)}\rangle = \frac{\sqrt{2}}{w}p_1(p_3+p_2), \tag{5.6d}$$

$$\langle \hat{P}^{1,3}_{(0,0)}+\hat{P}^{3,1}_{(0,0)}\rangle = \frac{\sqrt{2}}{w}p_1(p_3-p_2), \tag{5.6e}$$

$$\langle \hat{P}^{2,3}_{(0,0)}+\hat{P}^{3,2}_{(0,0)}\rangle = \frac{1}{w}(p_3^2-p_2^2), \tag{5.6f}$$

$$\sum_{\mu}\langle \hat{P}^{1,1}_{(4,\mu)}\rangle = \frac{w-h_1}{2wh_2}(p_4-p_5)^2, \tag{5.6g}$$

$$\sum_{\mu}\langle \hat{P}^{2,2}_{(4,\mu)}\rangle = \frac{w-h_1}{2wh_2}(p_4+p_5)^2, \tag{5.6h}$$

$$\sum_{\mu}\langle \hat{P}^{1,2}_{(4,\mu)}+\hat{P}^{2,1}_{(4,\mu)}\rangle = \frac{w-h_1}{wh_2}(p_4^2-p_5^2), \tag{5.6i}$$

$$\sum_{\mu}\langle \hat{P}^{0,0}_{(5,\mu)}\rangle = \frac{5p_6^2}{w}. \tag{5.6j}$$

These modifications of the model cause some changes in the ground-state phase diagram, e.g., the simple terms like Eqs. (5.6a) and (5.6j) will only shift the phase boundaries without changing the general structure of the phase diagram. Other interactions like the pair-hopping term (5.6f)

$$t_{pair}(d^{\dagger}_{\uparrow}d^{\dagger}_{\downarrow}c_{\uparrow}c_{\downarrow}+\text{H.c.}) \sim \hat{P}^{2,3}_{(0,0)}+\hat{P}^{3,2}_{(0,0)} \tag{5.7}$$

will dramatically change the phase diagram (see Fig. 7).

For small negative values of t_{pair} ($|t_{pair}| \leqslant t_{\parallel}$) the Ising-phase I of the phase diagram in Fig. 4 with the symmetric amplitude p_2 splits into two singlet phases: a symmetric (p_2) and an antisymmetric phase (p_3) [see Fig. 7(a) , $t_{pair}=-1$], where the crossover line has the same gradient ($U=-2V$). Increasing the amplitude of t_{pair} leads to a pure antisymmetric phase [see Fig. 7(b), $t_{pair}=-4$] in I and also to a strong change of the shape of the quartet phase. For small positive values of t_{pair} the general structure of the phase diagram is preserved (like Fig. 4). In the regime of the coupling constants with $t_{pair} \gg t_{\parallel}$ the quartet phase vanishes (see Fig. 8).

Other interactions also exhibit strong effects on the phase diagram, e.g., including a quartet term like (i) that contains a hopping term on a rung and a bond-charge interaction (see Appendix B).

$$t_{quar}[(c^{\dagger}_{\uparrow}d_{\uparrow}+\text{H.c.})\{1-(n_{c\downarrow}-n_{d\downarrow})^2\}+\uparrow \leftrightarrow \downarrow] \tag{5.8}$$

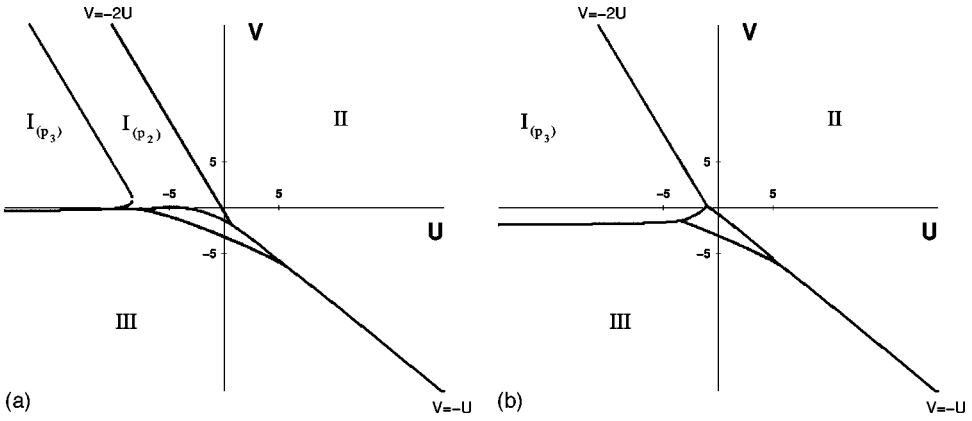

FIG. 7. Phase diagram for $t_\perp = 2t_\parallel$ including pair hopping for (a) $t_{pair} = -t_\parallel$ and (b) $t_{pair} = -4t_\parallel$ with $t_\parallel = 1$.

leads to different phase diagrams, depending on the coupling constant. For positive values of t_{quar} the quartet phase vanishes with increasing values of the coupling constant (like in Fig. 8) until there are only the three known phases [see Fig. 9(a)]. For $t_{quar} < 0$ the quartet phase grows [see Fig. 9(b)], dominated by the symmetric combination (p_4) of the states.

The mean deviation in the weak coupling limit in these two special cases (5.7) and (5.8) is small compared to the energy (calculated on a circle with radius $R = 0.1$ around $U = V = 0$) except for the value $t_{quar} \leqslant -1$. The ansatz also provides very good results in the strong-coupling limit ($R \geqslant 100$), except for the crossover lines to the superspin phase where the mean deviation is very large. The same problem occurs in the intermediate coupling regime in the quartet phase where the ansatz is not a good eigenstate of the system.

We expect that including the other interactions on a rung will lead to similar changes in the ground-state phase diagram.

2. Two-rung interactions

In most cases the SO(5)-symmetric interactions between two neighboring terms have a very complex structure but for some of them we can give simple expressions (see Appendix B). For them we can calculate the corresponding variational energy, e.g., the two-pair hopping term leading to an SO(5) singlet-singlet transition

$$t_{2\text{-}pair}[d_\uparrow^\dagger(x)d_\uparrow^\dagger(y)d_\downarrow^\dagger(x)d_\downarrow^\dagger(y)c_\uparrow(x) \times c_\uparrow(y)c_\downarrow(x)c_\downarrow(y) + \text{H.c.}] \tag{5.9}$$

giving $E_{two\text{-}pair} \sim 2t_{2\text{-}pair}(p_2+p_3)^2(p_3-p_2)^2$. The other SO(5)-singlet interactions on two rungs lead to similar expressions, which will change the phase diagram (Fig. 4) in the Ising phase according to the value of the coupling constant $t_{2\text{-}pair}$.

Including an SO(5)-quartet interaction in the SZH model [see Eq. (B18)] gives the variational energy

$$E = t_{qxy}\frac{w-h_1}{2wh_2(w+h_1)}(p_2^2-p_3^2)(p_4^2-p_5^2). \tag{5.10}$$

The phase diagrams obtained for different values of the coupling constant t_{qxy} are very similar to the phase diagram in Fig. 4. The additional interaction has no significant effect except for minor changes of the crossover lines.

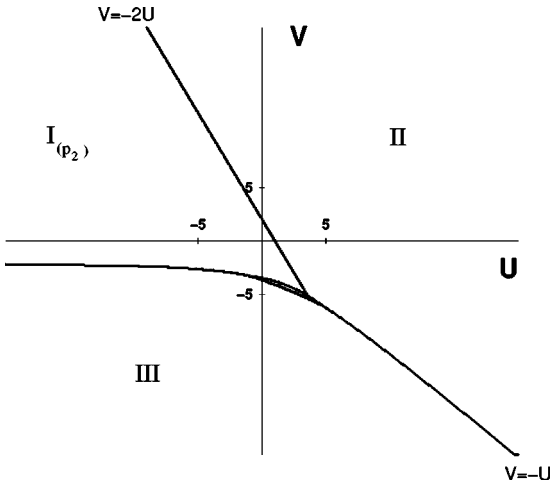

FIG. 8. Phase diagram for $t_\perp = 2t_\parallel$ including pair hopping for $t_{pair} = 4t_\parallel$ with $t_\parallel = 1$.

VI. SUMMARY AND OUTLOOK

We have constructed a large class of electronic ladder models with SO(5) symmetry having finitely correlated ground states and, consequently, correlation functions exhibiting exponential decay. These matrix-product states have been used to perform a variational study of the ground-state phase diagram of the SZH model[2] for $t_\perp \geqslant 2t_\parallel$. For vanishing coupling the ground state of the band insulator is found to be in the class of variational states and at strong coupling the phases identified by SZH are reproduced. In the intermediate coupling regime signatures of a new phase dominated by local SO(5) quartets are found, and at weak coupling the SO(5) superspin phase is absent. Within our approach it is possible to compute various correlations giving further insights into the nature of the phases that have been identified. Finally, we have introduced various SO(5) symmetric extensions to the SZH model and discussed their impact on the phase diagram. In the future we will include dimerization in the matrix-product ansatz for further studies of the Ising transition[2] in phase I and the possibility of spontaneous

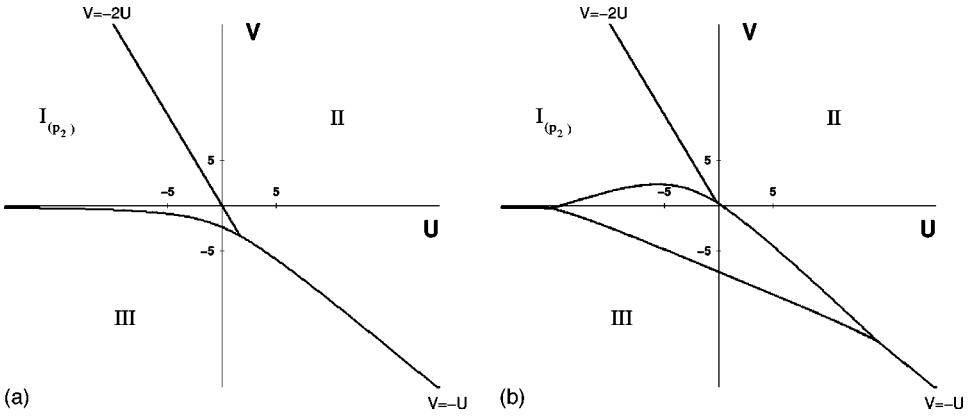

FIG. 9. Phase diagram for $t_\perp = 2t_\parallel$ including a quartet term with (a) $t_{quar} = +4t_\parallel$ and (b) $t_{quar} = -4t_\parallel$ with $t_\parallel = 1$.

breaking of translational invariance in exactly solvable models.

ACKNOWLEDGMENT

This work has been supported in part by the Deutsche Forschungsgemeinschaft under Grant No. Fr 737/3–1.

APPENDIX A: THE GAMMA MATRICES AND THE VARIATIONAL WAVE FUNCTION

For the construction of the SO(5)-invariant quantities, we have used the representation of the matrices in Ref. 2. The five Dirac Γ-matrices have the following form:

$$\Gamma^1 = \begin{pmatrix} 0 & -i\sigma_y \\ i\sigma_y & 0 \end{pmatrix}, \quad \Gamma^{2,3,4} = \begin{pmatrix} \vec{\sigma} & 0 \\ 0 & \vec{\sigma}^t \end{pmatrix}, \quad \Gamma^5 = \begin{pmatrix} 0 & \sigma_y \\ \sigma_y & 0 \end{pmatrix}, \tag{A1}$$

where $\vec{\sigma}$ are the Pauli matrices. The matrices Γ^{ab} are defined by $\Gamma^{ab} \equiv -i/2[\Gamma^a, \Gamma^b]$ and the matrix R is given by

$$R \equiv \begin{pmatrix} 0 & \mathbb{1} \\ -\mathbb{1} & 0 \end{pmatrix}. \tag{A2}$$

Using these definitions, it is simple to construct the matrix g_x of the variational wave function (4.1). It has the following structure

$$g_x = \left(\begin{array}{cccc|c} \multicolumn{4}{c|}{p_6 \Gamma^a n_a |\Omega\rangle + \sum_{i=1}^{3} p_i |\tilde{\Psi}^{(i)}_{0,0}\rangle \mathbb{1}} & \begin{matrix} |q_1\rangle \\ |q_2\rangle \\ |q_3\rangle \end{matrix} \\ & & & & |q_4\rangle \\ \hline -|q_3\rangle & -|q_4\rangle & |q_1\rangle & |q_2\rangle & 0 \end{array} \right). \tag{A3}$$

The three SO(5) singlets are included in this ansatz only on the main diagonal elements. $|\tilde{\Psi}^{(1)}_{0,0}\rangle \equiv |\Psi^{(1)}_{0,0}\rangle$ from (2.5) and $|\tilde{\Psi}^{(2,3)}_{0,0}\rangle$ are the symmetric and an antisymmetric combinations of the two other singlets

$$|\tilde{\Psi}^{(2,3)}_{0,0}\rangle = (\Psi^\dagger_\alpha R_{\alpha\beta} \Psi^\dagger_\beta \mp \Psi_\alpha R_{\alpha\beta} \Psi_\beta)|\Omega\rangle. \tag{A4}$$

The quartets enter the matrix g_x in $|q_\alpha\rangle = p_4 |Q^+_\alpha\rangle + p_5 |Q^-_\alpha\rangle$ where $|Q^\pm_\alpha\rangle$ are the symmetric and antisymmetric combinations of Eq. (2.7),

$$|Q^\pm_\alpha\rangle \sim \left\{ \left| \begin{matrix} \downarrow \\ - \end{matrix} \right\rangle \pm \left| \begin{matrix} - \\ \downarrow \end{matrix} \right\rangle, \left| \begin{matrix} \uparrow \\ - \end{matrix} \right\rangle \pm \left| \begin{matrix} - \\ \uparrow \end{matrix} \right\rangle, \left| \begin{matrix} \uparrow \\ \uparrow\downarrow \end{matrix} \right\rangle \pm \left| \begin{matrix} \uparrow\downarrow \\ \uparrow \end{matrix} \right\rangle, \left| \begin{matrix} \downarrow \\ \uparrow\downarrow \end{matrix} \right\rangle \pm \left| \begin{matrix} \uparrow\downarrow \\ \downarrow \end{matrix} \right\rangle \right\}. \tag{A5}$$

They are arranged in the right column and the lowest row of Eq. (A3) in such a way that in the product $g_x g_{x+1}$ one has SO(5) singlets on the diagonal only.

APPENDIX B: SO(5)-SYMMETRIC OPERATORS ON ONE (TWO) RUNGS

We present here a selection of various SO(5)-symmetric terms on a single and on two rungs (B1) and (B2). Furthermore, a list of terms is given for which our matrix-product ansatz (4.1) would be the lowest energy state (B3).

1. Single-rung interactions

We now present all possible SO(5)-symmetric terms on a rung. Their general construction is done in terms of projection operators on the different SO(5) multiplets. Expressed through electronic operators, most of them are already known from the SZH model (2.11) and an additional biquadratic exchange. As a shorthand notation we introduce

$$\begin{aligned} [U,V,J,\alpha] \equiv U\{[n_{c\uparrow}(x) - \tfrac{1}{2}][n_{c\downarrow}(x) - \tfrac{1}{2}] + (c \to d)\} \\ + V[n_c(x) - 1][n_d(x) - 1] + J\vec{S}_c(x)\vec{S}_d(x) \\ + \alpha[\vec{S}_c(x)\vec{S}_d(x)]^2. \end{aligned} \tag{B1}$$

In addition, we find various single-electron and pair-hopping terms together with bond-charge type interactions. Using the notation of Sec. II for the projection operators on a rung, we obtain the following terms by projection on the singlets

$$\hat{P}^{1,1}_{0,0} = |\Psi^{(1)}_{0,0}\rangle\langle\Psi^{(1)}_{0,0}| = \left[0, 0, -\frac{1}{3}, \frac{4}{3}\right], \tag{B2}$$

$$\hat{P}^{2,2}_{0,0}=\left[\frac{1}{2},-\frac{1}{4},\frac{2}{3},\frac{4}{3}\right]+\frac{1}{2}[n_{d\uparrow}n_{d\downarrow}(1-n_c)-c\leftrightarrow d], \tag{B3}$$

$$\hat{P}^{3,3}_{0,0}=\left[\frac{1}{2},-\frac{1}{4},\frac{2}{3},\frac{4}{3}\right]-\frac{1}{2}[n_{d\uparrow}n_{d\downarrow}(1-n_c)-c\leftrightarrow d], \tag{B4}$$

$$\hat{P}^{1,2}_{0,0}+\hat{P}^{2,1}_{0,0}=\frac{1}{\sqrt{2}}[(c^\dagger_\uparrow d_\uparrow+\text{H.c.})n_{d\downarrow}(n_{c\downarrow}-1)+\uparrow\leftrightarrow\downarrow], \tag{B5}$$

$$\hat{P}^{1,3}_{0,0}+\hat{P}^{3,1}_{0,0}=-\frac{1}{\sqrt{2}}[(c^\dagger_\uparrow d_\uparrow+\text{H.c.})n_{c\downarrow}[n_{d\downarrow}-1]+\uparrow\leftrightarrow\downarrow], \tag{B6}$$

$$\hat{P}^{2,3}_{0,0}+\hat{P}^{3,2}_{0,0}=d^\dagger_\uparrow d^\dagger_\downarrow c_\uparrow c_\downarrow+\text{H.c.} \tag{B7}$$

The projection operators on the quartet states read

$$\sum_{\mu=1}^{4}\hat{P}^{1,1}_{4,\mu}=\left[0,0,-\frac{8}{3},-\frac{16}{3}\right]+(1-n_{c\uparrow}n_{c\downarrow})n_d+n_{d\uparrow}n_{d\downarrow}(n_c-2), \tag{B8}$$

$$\sum_{\mu=1}^{4}\hat{P}^{2,2}_{4,\mu}=\left[0,0,-\frac{8}{3},-\frac{16}{3}\right]+(1-n_{d\uparrow}n_{d\downarrow})n_c+n_{c\uparrow}n_{c\downarrow}(n_d-2), \tag{B9}$$

$$\sum_{\mu=1}^{4}\hat{P}^{1,2}_{4,\mu}+\hat{P}^{2,1}_{4,\mu}=\{c^\dagger_\uparrow d_\uparrow+\text{H.c.})[1-(n_{c\downarrow}-n_{d\downarrow})^2]+\uparrow\leftrightarrow\downarrow\}, \tag{B10}$$

and finally, projection on the quintet gives

$$\sum_{\mu=1}^{5}\hat{P}_{5,\mu}=\left[1,\frac{1}{2},\frac{13}{3},\frac{20}{3}\right]. \tag{B11}$$

2. Interactions between neighboring rungs

Equivalently, the SO(5)-symmetric expressions on two rungs can be classified. The choice of the basis on the two-rung system is very important for the structure of the SO(5)-symmetric terms. Using the simplest combination, the product of an SO(5) singlet on one rung and another SO(5) multiplet on the other gives for a projection operator, e.g.,

$$\sum_{\mu=1}^{5}\hat{P}^{1,1}_{5,\mu}(x,y)=\hat{P}^{1,1}_{0,0}(x)\sum_{\mu=1}^{5}\hat{P}_{5,\mu}(y) \tag{B12}$$

for the product of an SO(5) singlet on rung x and an SO(5) quintet on y, where $\hat{P}^{k,l}_{d,\mu}$ is defined in Sec. II. The numbers k and l in $\hat{P}^{k,l}_{d,\mu}$ depend on the way the different multiplets on the rungs are labeled. Another example is an operator projecting on an SO(5) singlet on each of the rungs

$$\hat{P}^{2,2}_{0,0}(x,y)=|\Psi^{(2)}_{0,0}(x,y)\rangle\langle\Psi^{(2)}_{0,0}(x,y)|=\hat{P}^{1,1}_{0,0}(x)\hat{P}^{2,2}_{0,0}(y) \tag{B13}$$

[see Eq. (2.5) for the definition of the wave functions]. All projection operators of states consisting of at least one SO(5) singlet on a rung can be decomposed in the same manner. For some of these operators a compact representation in terms of electron operators is possible. As an example consider the operator

$$c^\dagger_\uparrow(x)c^\dagger_\downarrow(x)d^\dagger_\uparrow(y)d^\dagger_\downarrow(y)c_\uparrow(y)c_\downarrow(y)d_\uparrow(x)d_\downarrow(x)+\text{H.c.} \tag{B14}$$

describing pair exchange between two neighboring rungs. It causes a transition between two SO(5) singlet states and can be written as

$$\sim\hat{P}^{3,2}_{0,0}(y)\hat{P}^{3,2}_{0,0}(x)+\text{H.c.} \tag{B15}$$

Other SO(5) singlet-singlet transitions of this type are

$$\begin{aligned}&d^\dagger_\uparrow(x)d^\dagger_\uparrow(y)d^\dagger_\downarrow(x)d^\dagger_\downarrow(y)c_\uparrow(x)c_\uparrow(y)c_\downarrow(x)c_\downarrow(y)+\text{H.c.},\\&N_d(y)n_{c\uparrow}(y)n_{c\downarrow}(y)[d^\dagger_\uparrow(x)d^\dagger_\downarrow(x)c_\uparrow(x)c_\downarrow(x)+\text{H.c.}],\\&N_c(x)n_{d\uparrow}(x)n_{d\downarrow}(x)[c^\dagger_\uparrow(y)c^\dagger_\downarrow(y)d_\uparrow(y)d_\downarrow(y)+\text{H.c.}],\end{aligned} \tag{B16}$$

where

$$N_\alpha(y)=[1-n_{\alpha\uparrow}(y)-n_{\alpha\downarrow}(y)+n_{\alpha\uparrow}(y)n_{\alpha\downarrow}(y)],\qquad\alpha\in\{c,d\}. \tag{B17}$$

Similar terms are obtained from projection operators on direct products of an SO(5)-singlet on one and an SO(5) quartet on the other rung, e.g.,

$$\begin{aligned}&[([n_{c\uparrow}(x)-n_{d\uparrow}(x)]^2-1\}c^\dagger_\uparrow(y)c^\dagger_\downarrow(x)c^\dagger_\downarrow(y)d_\uparrow(y)d_\downarrow(x)d_\downarrow(y)\\&\quad+\{[n_{c\downarrow}(x)-n_{d\downarrow}(x)]^2-1\}\\&\quad\times c^\dagger_\uparrow(x)c^\dagger_\uparrow(y)c^\dagger_\downarrow(y)d_\uparrow(x)d_\uparrow(y)d_\downarrow(y)]+\text{H.c.}\end{aligned} \tag{B18}$$

The projection operators on the remaining 169 states with a structure similar to Eq. (3.3) cannot easily be decomposed in this way. They are significantly more complex, generically their expansion into electronic operators produces complicated bond-charge interaction terms. Still, forming suitable linear combinations of such terms can lead to simpler SO(5)-symmetric terms on two rungs, e.g., the pair-hopping term in Eq. (3.1) or a diagonal hopping term

$$\sum_{\langle x,y\rangle}[d^\dagger_\sigma(x)c_\sigma(y)-c^\dagger_\sigma(x)d_\sigma(y)+\text{H.c.}].$$

3. SO(5)-symmetric Hamiltonians with exact ground states

At the end of Sec. IV we claimed that a general Hamiltonian where our ansatz (4.1) is the ground state of the system is given by

$$h_{x,x+1}=\sum_{k,l=1}^{4}\lambda_{16}^{(k,l)}\sum_{\mu=1}^{16}\hat{P}_{16,\mu}^{k,l}+\sum_{\mu=1}^{14}\lambda_{14}\hat{P}_{14,\mu}$$
$$+\text{additional terms.} \tag{B19}$$

The coupling constants have to be chosen such that $\lambda_{14}>0$ and the matrix λ_{16} of coupling constants is positive definite. This implies that $E=0$ is a lower bound on the spectrum and therefore the state (4.1)—having zero energy by construction—will be a ground state. The additional terms in Eq. (B19) are the projection operators on the remaining multiplets, not present in the matrix-product wave function. For example, the projection operator on one of the SO(5) singlets not present in this product reads

$$\lambda_0^{(k,l)}[-c_\uparrow^\dagger(x)c_\uparrow^\dagger(y)c_\downarrow^\dagger(x)c_\downarrow^\dagger(y)d_\uparrow(x)d_\uparrow(y)d_\downarrow(x)d_\downarrow(y)$$
$$+n_{d\uparrow}(x)n_{d\uparrow}(y)n_{d\downarrow}(x)n_{d\downarrow}(y)N_c(x)N_c(y)+(c\leftrightarrow d)]. \tag{B20}$$

Just as λ_{16} above, the matrices λ_d, $d=0,4,5,10$ coupling the projection operators on the remaining multiplets have to be chosen to be positive definite.

APPENDIX C: CORRELATION FUNCTIONS

The calculation of expectation values between matrix-product states is straightforward using a transfer matrix method (see, e.g., Ref. 22).

To this end we define a 25×25 transfer matrix G on a rung

$$G_{\alpha_1,\alpha_2}\sim G_{(i_1,j_1),(i_2,j_2)}\equiv g^\dagger_{(i_1,i_2)}g_{(j_1,j_2)} \tag{C1}$$

with the indices

$$\alpha_1=1,\ldots,25\leftrightarrow(11),\ldots,(15),(21),\ldots,(55).$$

In terms of G the norm of the ground state can be written as

$$\langle\Psi_0|\Psi_0\rangle=\mathrm{Tr}\,G^L=\sum_{i=1}^{25}\lambda_i^L, \tag{C2}$$

where λ_i are the eigenvalues of G. In the thermodynamic limit ($L\to\infty$) the largest eigenvalue λ_1 dominates this expression and we obtain $\langle\Psi_0|\Psi_0\rangle\sim\lambda_1^L$. Similarly, one-point correlators of an operator O are

$$\langle O\rangle=\frac{1}{\lambda_1}\langle e_1|Z(O)|e_1\rangle \tag{C3}$$

and a two-point correlation function reads

$$\langle O_1^\dagger O_r\rangle=\sum_{n=1}^{25}\frac{1}{\lambda_n^2}\left(\frac{\lambda_n}{\lambda_1}\right)^r\langle e_1|Z(O_1)|e_n\rangle\langle e_n|Z(O_r)|e_1\rangle. \tag{C4}$$

Here $|e_n\rangle$ are the eigenvectors with eigenvalue λ_n of G and $Z(O_i)\sim g^\dagger O_i g$ is the transfer matrix related to the operator O_i. With the matrix (A3) the largest eigenvalue of G is given by

$$\lambda_1=\frac{1}{2}(h_1+w) \tag{C5}$$

with

$$h_1=5p_6^2+p_1^2+p_2^2+p_3^2,\quad h_2=p_4^2+p_5^2,$$

and

$$w=\sqrt{h_1^2+16h_2^2}.$$

This enables us to calculate the expectation values of any operator acting on a single or two rungs, respectively. For example, we find

$$\langle\vec{S}\rangle=0,\quad \langle(S^i)^2\rangle=\frac{w-h_1+8p_6^2}{4w} \tag{C6}$$

for local magnetic moments and

$$\langle c_{g(u)}^\dagger(x)c_{g(u)}(x)\rangle=\frac{1}{w}\left[\frac{w-h_1}{h_2}(p_5^2+3p_4^2)+2h_1\mp4p_1p_2\right], \tag{C7}$$

$$\langle c_\alpha^\dagger(x)c_\beta(x)\rangle=\frac{1}{w}\left[\frac{w-h_1}{h_2}(2p_4p_5)-4p_2p_3\right],\quad \alpha\neq\beta \tag{C8}$$

for electronic expectation values. Here, $\alpha,\beta\in\{g,u\}$ and $c_{g,u}(x)=[c_\uparrow(x)+c_\downarrow(x)]\pm[d_\uparrow(x)+d_\downarrow(x)]$.

Correlations between the total spin on two rungs decay exponentially

$$\langle\vec{S}_1\vec{S}_r\rangle=-\frac{3}{4w(h_1+w)}\left(\frac{h_1-4p_6^2}{\lambda_1}\right)^r\left(\frac{w-h_1+8p_6^2}{h_1-4p_6^2}\right)^2 \tag{C9}$$

as expected for finitely correlated states. Spin-spin correlations between individual sites on rungs separated by a distance r can be expressed as

$$\langle\vec{S}_\alpha(r)\vec{S}_\beta(0)\rangle=A_{\alpha\beta}(\{p_i\})\left(\frac{h_1-4p_6^2}{\lambda_1}\right)^r$$
$$+B_{\alpha\beta}(\{p_i\})\left(\frac{h_1-8p_6^2}{\lambda_1}\right)^r, \tag{C10}$$

where the amplitudes $A_{\alpha\beta}(\{p_i\})$ and $B_{\alpha\beta}(\{p_i\})$ depend on the choice of α and β, i.e., whether correlators of spins on the same or on different legs of the ladder are considered. Analogously, one can study electronic correlations, e.g.,

$$\langle c_g^\dagger(r)c_u^\dagger(r)c_g(0)c_u(0)\rangle=-\frac{8}{3}\langle\vec{S}_1\vec{S}_r\rangle,$$

$$\langle c_{g,u}^\dagger(r)c_{g,u}(0)\rangle=C_{g,u}(\{p_i\})\left(\frac{h_2}{\lambda_1}\right)^r+D_{g,u}(\{p_i\})\left(-\frac{h_2}{\lambda_1}\right)^r, \tag{C11}$$

with the amplitudes $C_{g,u}$ and $D_{g,u}$.

[1] S. Zhang, Science **275**, 1089 (1997).
[2] D. Scalapino, S. Zhang, and W. Hanke, Phys. Rev. B **58**, 443 (1998).
[3] D. G. Shelton and D. Sénéchal, Phys. Rev. B **58**, 6818 (1998).
[4] H. Lin, L. Balents, and M. Fisher, Phys. Rev. B **58**, 1794 (1998).
[5] E. Dagotto and T. M. Rice, Science **271**, 618 (1996).
[6] I. Affleck, T. Kennedy, E. H. Lieb, and H. Tasaki, Phys. Rev. Lett. **59**, 799 (1987).
[7] M. Fannes, B. Nachtergaele, and R. Werner, Europhys. Lett. **10**, 633 (1989).
[8] A. Klümper, A. Schadschneider, and J. Zittartz, J. Phys. A **24**, L955 (1991).
[9] M. Nakamura, Phys. Rev. B **61**, 16 377 (2000).
[10] M. Nakamura, K. Itoh, and N. Muramoto, cond-mat/0003419 (unpublished).
[11] D. Dmitriev, V. Krivnov, and A. Ovchinnikov, Phys. Rev. B **61**, 14 592 (2000).
[12] E. H. Kim, G. Sierra, and D. Duffy, Phys. Rev. B **60**, 5169 (1999).
[13] A. Kolezhuk and H.-J. Mikeska, Int. J. Mod. Phys. B **12**, 2325 (1998).
[14] S. Brehmer, A. K. H.-J. Mikeska, and U. Neugebauer, J. Phys.: Condens. Matter **10**, 1103 (1998).
[15] U. Neugebauer and H.-J. Mikeska, Z. Phys. B; Condensed Matter **99**, 151 (1996).
[16] K. Totsuka and M. Suzuki, J. Phys.: Condens. Matter **7**, 1639 (1995).
[17] S. Rabello, H. Kohno, E. Demler, and S.-C. Zhang, Phys. Rev. Lett. **80**, 3586 (1998).
[18] A. Kolezhuk and H.-J. Mikeska, Phys. Rev. B **56**, R11 380 (1997).
[19] A. Kolezhuk and H.-J. Mikeska, Eur. Phys. J. B **5**, 543 (1998).
[20] S. Brehmer, H.-J. Mikeska, and U. Neugebauer, J. Phys.: Condens. Matter **8**, 7161 (1996).
[21] A. Kolezhuk and H.-J. Mikeska, Phys. Rev. Lett. **80**, 2709 (1998).
[22] A. Klümper, A. Schadschneider, and J. Zittartz, Z. Phys. **87**, 281 (1992).
[23] V. Emery, S. Kivelson, and O. Zachar, Phys. Rev. B **59**, 15 641 (1999).